Journal of Institute of Science and Technology, 31(1), 107-118 (2026)
ISSN: 2467-9062 (print), e-ISSN: 2467-9240
https://doi.org/10.3126/jist.v31i1.88693

Research Article

PERFORMANCE ANALYSIS OF EMPIRICAL MODELS FOR ESTIMATING DAILY GLOBAL SOLAR RADIATION AT TAPLEJUNG, NEPAL

Basanta Kumar Rajbanshi[1]*, Ram Gopal Singh[1], Anima Kumari Singh Rajbanshi[2], Bed Raj KC[3]

[1]*Department of Physical Sciences, Shri Ramswaroop Memorial University, Devaroad-Lucknow, Barabanki, India*
[2]*Department of Chemistry, Tri-Chandra Campus, Tribhuvan University, Kathmandu, Nepal*
[3]*Pokhara University, Kaski, Gandaki Province, Nepal*
**Correspondence*: basantaraz05@gmail.com

(***Received:*** *December 31, 2025;* ***Revised:*** *March 7, 2026;* ***Accepted:*** *May 30, 2026)*

ABSTRACT

Accurate knowledge of global solar radiation (GSR) is a fundamental requirement for solar energy system design, climate studies, and environmental modeling. In mountainous regions such as eastern Nepal, the scarcity of long-term measured solar radiation data necessitates the use of empirical estimation techniques. This study presents a comprehensive evaluation of twenty empirical models for estimating daily average GSR on a horizontal surface for Taplejung, a high-altitude region of Nepal. The models were calibrated using locally observed meteorological data, and their performance was assessed through standard statistical indicators, including Mean Bias Error (MBE), Root Mean Square Error (RMSE), Mean Percentage Error (MPE), and the coefficient of determination (R^2). The comparative analysis reveals substantial variation in predictive performance among the tested formulations. Advanced multivariable and nonlinear models significantly outperform simpler regression relations. Among all models, the Coulibaly and Ouedraogo model demonstrates the most balanced performance, characterized by near-zero bias, low dispersion error, and the highest correlation strength. The results confirm that Taplejung possesses a notable solar energy potential, with an estimated mean daily GSR of approximately 15.12 MJ m^{-2} day^{-1}. The proposed findings provide a reliable framework for solar resource assessment in high-altitude regions of Nepal where direct measurements are limited.

Keywords: Empirical models, Global solar radiation, Mountain climate, Statistical evaluation, Taplejung

INTRODUCTION

The growing demand for sustainable and low-carbon energy resources has intensified global interest in solar energy as a clean and renewable alternative to fossil fuels. Solar radiation is the primary driver of photovoltaic and solar thermal systems and plays a crucial role in climate processes, hydrology, and agricultural productivity. Reliable estimation of global solar radiation (GSR) is therefore essential for energy planning, system optimization, and environmental studies (Iqbal, 1983; Badescu, 2008).

In many developing countries, including Nepal, direct and continuous measurement of solar radiation is limited due to the high cost of instrumentation, maintenance requirements, and uneven spatial distribution of meteorological stations. These challenges are amplified in mountainous and remote regions where complex terrain and harsh climatic conditions restrict long-term observational records (Adhikari et al., 2013; Poudyal, 2015). As a result, empirical models that estimate GSR using commonly available meteorological parameters such as sunshine duration, air temperature, relative humidity, and rainfall have become practical and widely used alternatives (Ampratwum & Dorvlo, 1999; Ertekin & Yaldiz, 2000).

A wide range of empirical formulations has been developed and applied across different climatic regions of the world. Numerous comparative studies have shown that model performance is highly dependent on local climatic conditions, altitude, and atmospheric transparency (Evrendilek & Ertekin, 2008; Sonmete et al., 2011; Trnka et al., 2005). In mountainous environments, rapid cloud formation, strong temperature gradients, and variable aerosol loading often reduce the accuracy of simple regression-based models, highlighting the necessity of site-specific calibration and multi-model evaluation (Dogniaux & Lemoine, 1983; Okundamiya et al., 2016).

Nepal presents exceptional geographical and climatic diversity, ranging from the low-lying Terai plains to mid-hill regions and the high Himalayan belt. Several studies have evaluated empirical GSR models in Nepal, primarily focusing on lowland and mid-hill locations (Poudyal et al., 2012; Joshi et al., 2020). More recent investigations have extended these analyses to upland and high-altitude regions using multi-parameter approaches and advanced computational tools, demonstrating that model suitability varies significantly with elevation and climatic regime (Rajbanshi et al., 2024a, 2024b; Kharel et al., 2025).

Recent studies published in 2025 indicate a growing trend toward hybrid and advanced empirical approaches that integrate multiple meteorological variables and nonlinear relationships to improve estimation accuracy. These models have shown superior performance compared to traditional formulations, particularly in regions characterized by complex atmospheric dynamics (Hamatti, et al., 2025; Kharel et al., 2025; Rajbanshi et al., 2025a & 2025b; Although machine-learning-based techniques are increasingly explored, empirical and hybrid models remain attractive due to their transparency, lower data requirements, and ease of implementation (Tanyıldızı Ağır, 2025; Yadav et al., 2025).

Taplejung, located in the eastern Himalayan uplands of Nepal, represents a climatically distinct region characterized by high elevation, strong seasonal variability, and rapidly changing atmospheric conditions. Despite its substantial solar energy potential, long-term measured GSR data for this region remain scarce. A systematic evaluation of empirical models under such conditions is therefore necessary to support reliable solar resource assessment and decentralized energy planning.

The objective of this study is to conduct a comprehensive comparative assessment of twenty widely used empirical models for estimating daily global solar radiation on a horizontal surface in Taplejung, Nepal. Using locally observed meteorological data, the models are calibrated and evaluated through multiple statistical indicators to identify the most reliable formulation for high-altitude Himalayan environments. The findings aim to contribute to improved solar energy planning and environmental modeling in eastern Nepal and similar mountainous regions where direct radiation measurements are limited.

MATERIALS AND METHODOLOGY

Study area

Taplejung District is located in eastern Nepal within Koshi Province, extending between approximately 27.06°–27.55°N latitude and 87.23°–88.08°E longitude (Fig. 1). The district covers about 3,646 km² and exhibits remarkable altitudinal variation from about 670 m to 8,586 m above mean sea level, including Mount Kanchenjunga. The terrain is predominantly rugged and mountainous, characterized by steep slopes, deep valleys, dense forests, and alpine landscapes. Major river systems such as the Tamor River drain the region.

Figure 1. Map of Nepal indicating the highlighted study area of Taplejung

Taplejung experiences a high-altitude mountainous climate with cool temperatures and strong seasonal variation influenced by the monsoon. Winters are cold and dry, while summers are mild with frequent cloud cover and precipitation. Higher atmospheric transparency during non-monsoon months enhances solar radiation availability, making the district suitable for evaluating empirical Global Solar Radiation (GSR) models under complex mountain conditions.

Meteorological data

Meteorological data for Taplejung were obtained from the Department of Hydrology and Meteorology, Government of Nepal, Babarmahal, Kathmandu. The dataset spans the period from 2020 to 2023 and comprises daily maximum temperature (Tmax), daily minimum temperature (Tmin), sunshine duration, rainfall, hourly global solar radiation (GSR), relative humidity recorded at three-hour intervals, and wind speed measured at three-hour intervals. Data quality control procedures were performed prior to analysis, including screening for missing values and inconsistencies, to ensure the accuracy and reliability of the dataset.

Empirical models

A total of twenty empirical models were selected from the literature for evaluation. These models represent a wide range of functional forms, including linear, polynomial, exponential, and multivariable regression relations. The general structure of the models involves empirical constants (a–f) that were calibrated using regression analysis based on local data.

Astronomical parameters

Standard astronomical relations were used to compute extraterrestrial solar radiation, solar declination, sunset hour angle, and maximum possible sunshine duration. These parameters form the basis of many sunshine-based empirical models and ensure physical consistency across formulations.

Declination angle (δ)

The declination angle is the angle between the Earth–Sun line and the Earth's equatorial plane. This angle varies throughout the year, ranging from 23.45° during the winter solstice to +23.45° at the summer solstice. It can be estimated using the following equation

$$(\delta \text{ degree}) = 23.45\sin\left[\frac{360}{365}(284 + n_d)\right] \qquad (1)$$

where n_d is the number of days corresponding to a given date, starting from 1 on 1 January to 365 on 31 December.

Sunset hour angle (ω)

The sunset hour angle in degrees can be calculated from;

$$\omega = \cos^{-1}(-\tan\phi \tan\delta) \qquad (2)$$

Number of daylight hours (daylight duration)

The duration of daylight (total hours of sunlight) depends on the hour angle and can be calculated using the following equation:

$$N = \frac{2}{15}\omega = \frac{2}{15}\cos^{-1}(-\tan\phi \tan\delta) \qquad (3)$$

Extraterrestrial radiation

The extraterrestrial GSR (Ho) can be calculated from the following equations:

$$H_0 = \frac{24}{\pi} I_{sc}\left[1 + 0.033\cos\left(\frac{360 n_d}{365}\right)\right]\left[\cos\phi \cos\delta \sin\omega + \frac{\pi}{180}\omega \sin\phi \sin\delta\right] \qquad (4)$$

Where,
I_{sc} = solar constant (=1367 W m^{-2}),
φ = the latitude of the site (rad),
Δ = the solar declination (rad),
Ω = the mean sunrise hour angle for the given month, and
n_d = the Julian day number of the year starting from the first of January.

Table 1. Set of models used in this study (Angstrom, 1924; Prescott, 1940; Chen et al., 2004; Khalil & Shaffie, 2014; Olomiyesan et al., 2017; Gairaa & Bakelli, 2013; Ögelman et al., 1984)

S.N.	Models	Mathematical Relations
M-1	Angstrom-Prescott-Page	$\frac{H_g}{H_0} = a + b\left(\frac{n}{N}\right)$
M-2	Temperature based Model	$\frac{H_g}{H_0} = a + bT_1$

M-3	Humidity based Model	$\frac{H_g}{H_0} = a + b\,RH$
M-4	Garica model (1994)	$\frac{H_g}{H_0} = a + b\left(\frac{\Delta T}{N}\right)$
M-5	Ampratwum and Dorvlo model	$\frac{H_g}{H_0} = a + b * \log\left(\frac{n}{N}\right)$
M-6	Chen et al. model 1	$\frac{H_g}{H_0} = a + b * \ln(\Delta T)$
M-7	Modified Angstrom Model	$\frac{H_g}{H_0} = a + b\left(\frac{n}{N}\right) + c(\Delta T)$
M-8	Swartzman-Ogunlade 2	$\frac{H_g}{H_0} = a + b\left(\frac{n}{N}\right) + c(RH)$
M-9	Newland model	$\frac{H_g}{H_0} = a + b\left(\frac{n}{N}\right) + c * \log\left(\frac{n}{N}\right)$
M-10	Modified Angstrom Model	$\frac{H_g}{H_0} = a + b\left(\frac{n}{N}\right) + c(T_1)$
M-11	Olomiyesan-Oyedum Model	$\frac{H_g}{H_0} = a + b\left(\frac{n}{N}\right) + c\left(\frac{\Delta T}{N}\right)$
M-12	Abdalla model	$\frac{H_g}{H_0} = a + b\left(\frac{n}{N}\right) + c(T_1) + d(RH)$
M-13	Togrul and Onat model 1	$H_g = a + b\left(\frac{n}{N}\right) + c\sin\delta + dT$
M-14	Modified Angstrom (new) Model	$\frac{H_g}{H_0} = a + b\left(\frac{n}{N}\right) + c(\Delta T) + d(RH)$
M-15	Modified Angstrom (new) Model	$\frac{H_g}{H_0} = a + b\left(\frac{n}{N}\right) + c\left(\frac{\Delta T}{N}\right) + d(RH)$
M-16	Chen et al. model 2	$H_g = a + b\left(\frac{n}{N}\right) + c\sin\delta + dT_{max}$
M-17	Ododo et al. Model	$H_g = a + b\left(\frac{n}{N}\right) + cT_{max} + d(RH) + eT_{max}\left(\frac{n}{N}\right)$
M-18	Togrul and Onat model 3	$H_g = a + b\left(\frac{n}{N}\right) + c\sin\delta + dT + e(RH)$
M-19	Togrul and Onat model 2	$H_g = a + bH_0 + c\left(\frac{n}{N}\right) + d\sin\delta + eT + f(RH)$
M-20	Coulibaly and Ouedraogo Model	$H_g = a + bH_0 + c\left(\frac{n}{N}\right) + d(RH) + eT_{max} + f\sin\delta$

Statistical performance indicators

The performance of the empirical models was evaluated using four standard statistical indicators commonly applied in solar radiation studies. Mean Bias Error (MBE) was used to identify systematic overestimation or underestimation of global solar radiation. Root Mean Square Error (RMSE) quantifies the spread of prediction errors and reflects overall estimation accuracy. Mean Percentage Error (MPE) assesses the relative deviation between estimated and observed values, while the coefficient of determination (R^2) indicates the proportion of variance in measured data explained by each model. A model is considered reliable when it simultaneously exhibits minimal bias (MBE close to zero), low RMSE and MPE values, and a high R^2, reflecting both accuracy and strong explanatory capability. The mathematical expressions for these metrics are provided below in Table 2 (Angstrom, 1924; Prescott, 1940; Gairaa & Bakelli, 2013).

Table 2. Statistical indicators used for analysis

Metrics	Relations	Units	Explanations
Mean percentage error (MPE)	$\text{MPE} = \frac{1}{N}\left[\sum\left(\frac{H_{i,c}-H_{i,m}}{H_{i,m}}\right)\times 100\right]$	%	The MPE represents the average percentage difference between the estimated and observed solar radiation values. Here, *N* denotes the total number of data pairs used for comparison.

Mean bias Error (MBE)	$\text{MBE} = \frac{1}{N}\sum(H_{i,c} - H_{i,m})$	MJ/m^2/day	The MBE reflects the average deviation between the measured and estimated values. It provides insight into the long-term accuracy of a model or correlation.
Root mean square error (RMSE)	$\text{RMSE} = \sqrt{\frac{1}{N}\sum(H_{i,c} - H_{i,m})^2}$	MJ/m^2/day	The RMSE serves as a general measure of the short-term accuracy of the models. Since RMSE values are always positive, a smaller RMSE indicates higher model accuracy. Ideally, an RMSE value of zero represents a perfect fit.
Correlation Coefficient (R^2)	$R^2 = \sum_{k=0}^{n}\binom{n}{k}x^k a^{n-k} = \frac{\sum(H_{i,m}-\overline{H_m})(H_{i,c}-\overline{H_c})}{\sqrt{\sum(H_{i,m}-\overline{H_m})^2(H_{i,c}-\overline{H_c})^2}}$	%	The correlation coefficient is employed to assess the relationship between the estimated and observed values. Here, c_a and m_a represent the mean values of the calculated and measured data, respectively.

Where,

$H_{i,\,m}$ = measured value,
$H_{i,\,c}$ = estimated value, is the number of data,
$\overline{H_m}$= the average of measured solar radiation,
$\overline{H_c}$= the average of estimated solar radiation.

RESULTS

Empirical constants and statistical indicators

The calibrated empirical constants and corresponding statistical indicators for the twenty empirical models are summarized in Table 3**.** The estimated mean daily global solar radiation (GSR) values obtained from all models vary within a narrow range of 15.10 -15.16 MJ m^{-2} day^{-1}**,** indicating strong consistency in long-term solar radiation availability over Taplejung. This narrow spread suggests that, despite differences in mathematical formulation and predictor variables, all models converge toward a similar annual mean solar resource. Such consistency reflects the dominant influence of regional climatic and topographic controls, particularly altitude and atmospheric transparency, on long-term solar radiation receipt in the study area.

Table 3. The empirical constants and statistical tools for different models for Taplejung

Models	Empirical constants						Statistical tools				
	a	**b**	**c**	**d**	**e**	**f**	**MBE (MJ/m^2/day)**	**RMSE (MJ/m^2/day)**	**MPE (%)**	**R^2**	**Hest**
M1	0.28	0.43					-0.05	4.11	14.29	0.43	15.11
M2	0.11	0.02					-0.05	5.05	21.82	0.15	15.11
M3	1.03	-0.01					-0.05	4.80	20.61	0.22	15.11
M4	0.16	0.40					-0.04	4.56	15.86	0.29	15.12
M5	0.57	0.22					-0.05	4.81	22.27	0.23	15.11
M6	-0.20	0.31					-0.05	1.65	10.18	0.36	15.11
M7	0.22	0.35	0.01				-0.05	1.66	13.11	0.44	15.11
M8	0.29	0.42	-0.00				-0.05	4.11	14.31	0.43	15.11
M9	0.29	0.39	0.00				-0.05	4.60	21.28	0.30	15.11
M10	-0.04	0.51	0.02				-0.05	3.48	9.57	0.59	15.11
M11	0.26	0.39	0.05				-0.05	4.10	13.95	0.43	15.11
M12	0.11	0.36	0.02	-0.00			-0.05	3.23	7.41	0.64	15.11
M13	6.80	10.73	1.09	0.37			-0.00	3.98	13.09	0.47	15.16

M14	-0.01	0.36	0.02	0.00			-0.05	4.04	12.38	0.45	15.11
M15	0.22	0.40	0.06	0.00			-0.05	4.10	13.87	0.43	15.11
M16	-4.11	14.18	1.34	0.59			-0.00	3.22	8.09	0.65	15.16
M17	0.19	0.16	0.02	-0.00	0.01		-0.05	3.21	8.27	0.64	15.11
M18	-0.39	11.30	1.17	0.56	0.07		0.00	3.96	12.36	0.47	15.16
M19	-2.24	0.06	11.33	1.28	0.56	0.07	0.00	3.95	12.38	0.47	15.16
M20	2.87	0.03	11.11	-0.1	0.65	1.01	-0.00	3.12	7.69	0.67	15.16

Comparative performance of empirical models

A comprehensive comparison of model performance is presented in Table 2, using Mean Bias Error (MBE), Root Mean Square Error (RMSE), Mean Percentage Error (MPE), coefficient of determination (R^2), and estimated mean GSR (Hest). All models were calibrated using locally observed meteorological data from Taplejung, a high-altitude mountainous region of eastern Nepal.

Across all formulations, the estimated mean daily GSR remains clustered around 15.12 MJ m^{-2} day^{-1}, indicating stable long-term solar availability. However, notable differences are observed in short-term predictive accuracy and variability representation, highlighting the importance of rigorous statistical evaluation.

Bias characteristics (MBE)

The MBE analysis reveals that most empirical models exhibit a negative bias, indicating a slight tendency to underestimate measured GSR. Models M1–M12 show MBE values close to –0.05 MJ m^{-2} day^{-1}, representing systematic but relatively small underprediction.

Such underestimation is commonly reported in mountainous regions, where rapid cloud development, variable atmospheric thickness, and complex terrain-induced effects are difficult to fully capture using simple regression-based approaches.

In contrast, advanced formulations **(**M13, M16, and M18–M20**)** demonstrate near-zero bias, with MBE values of the order of 10^{-7}–10^{-6} MJ m^{-2} day^{-1}**.** This improvement is attributed to the inclusion of multiple meteorological parameters and nonlinear interaction terms, which enhance bias correction and long-term accuracy.

Error dispersion and predictive accuracy

The RMSE values across the twenty models range from 1.65 MJ m^{-2} day^{-1} to more than 5.0 MJ m^{-2} day^{-1}, indicating substantial variation in short-term estimation performance. The lowest RMSE values are obtained for: M6**:** 1.65 MJ m^{-2} day^{-1} and M7**:** 1.66 MJ m^{-2} day^{-1}.

These models significantly outperform simple sunshine-duration-based formulations, demonstrating the benefit of incorporating additional meteorological variability in complex terrains. Models M12, M16, M17, and M20 also exhibit strong predictive capability, with RMSE values close to 3.2 MJ m^{-2} day^{-1}. Conversely, models M2, M3, M5, and M9 show RMSE values exceeding 4.5 MJ m^{-2} day^{-1}, indicating limited suitability for operational solar resource assessment in Taplejung. The MPE results further support these findings, with M10, M12, M17, and M20 recording single-digit percentage errors, reflecting minimal relative deviation from observed values.

Correlation strength (R^2)

The coefficient of determination (R^2) provides insight into the ability of each model to reproduce observed variability in daily GSR. Simple two-parameter models generally yield low R^2 values ($\leq$ 0.30), indicating insufficient explanatory power under highly variable mountain meteorological conditions. In contrast, multivariable and nonlinear formulations demonstrate a clear improvement. The highest R^2 values are obtained for:

M20**:** R^2 = 0.671, M16**:** R^2 = 0.651, M17**:** R^2 = 0.639, M12**:** R^2 = 0.636

These results indicate that more than 65% of the observed variance in daily GSR can be explained by advanced empirical formulations, underscoring their suitability for high-altitude environments.

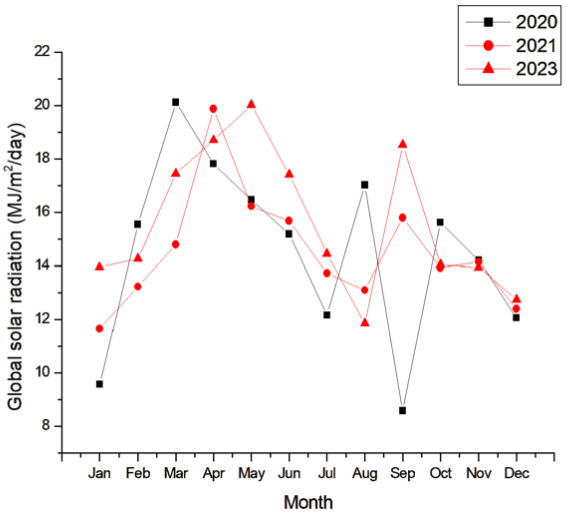

Figure 2. Variation of measured monthly average daily global solar radiation for 2020, 2022 and 2023

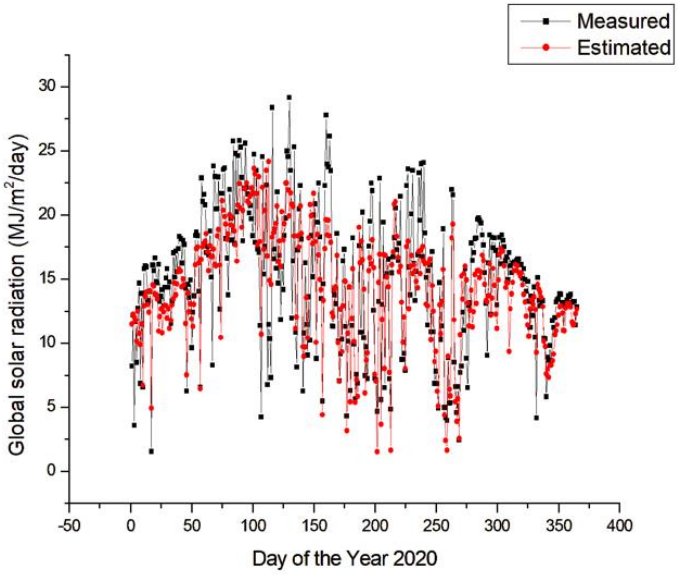

Figure 3. Graphic representation of the variation of measured and estimated daily global solar radiation for 2020

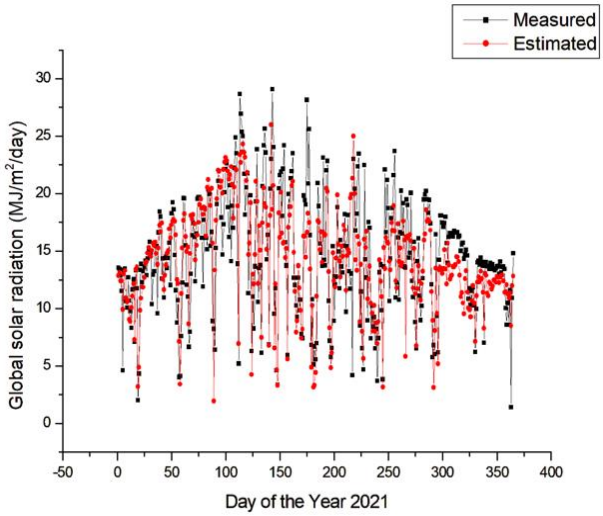

Figure 4. Graphic representation of the variation of measured and estimated daily global solar radiation for 2021

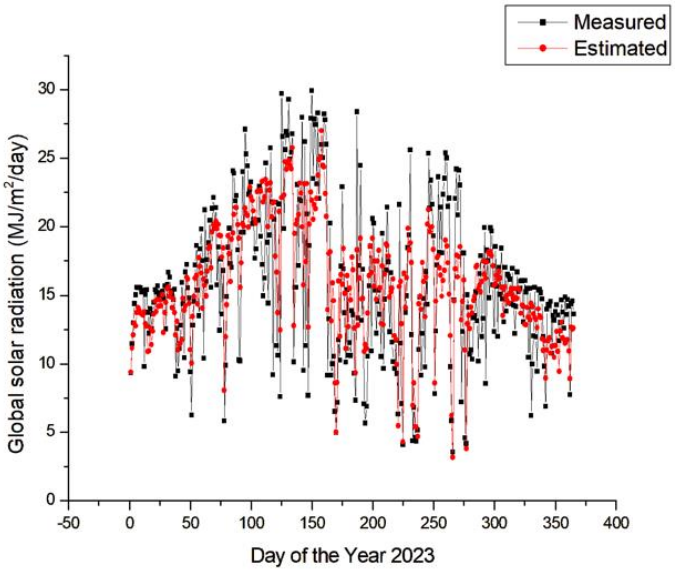

Figure 5. Graphic representation of the variation of measured and estimated daily global solar radiation for 2023

Selection of optimal models

Considering all statistical indicators collectively-near-zero MBE, minimum RMSE and MPE, and maximum R^2 Model M20 (Coulibaly and Ouedraogo) emerges as the most reliable formulation for Taplejung. It demonstrates: Negligible systematic bias, low prediction error, strong correlation with measured data, and physically consistent estimated mean GSR. Models **M**16 and M17 also exhibit strong performance and may serve as practical alternatives where data availability restricts the use of more complex inputs.

It is noteworthy that models with very low RMSE but moderate R^2 (e.g., M6 and M7) illustrate that low error alone does not guarantee strong explanatory power, highlighting the importance of multi-criteria evaluation.

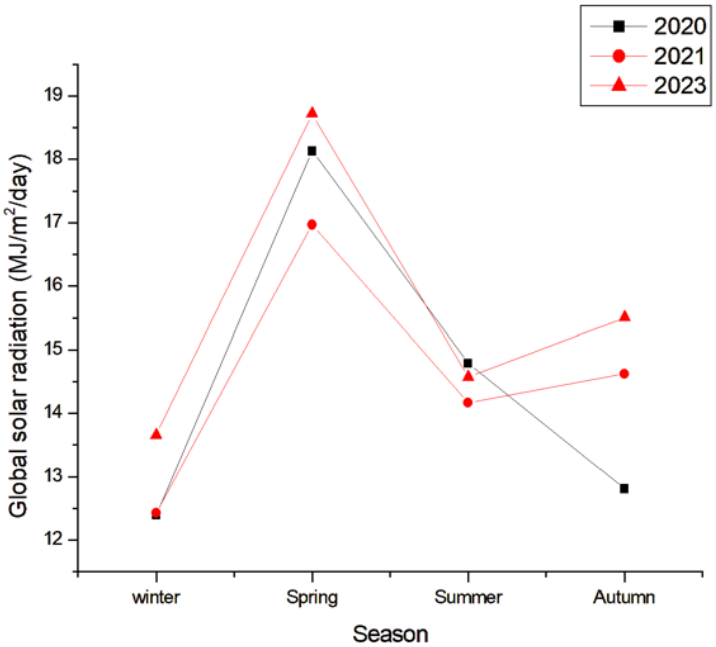

Figure 6. Graphic representation of the variation of seasonal global solar radiation for 2020, 2021 and 2023

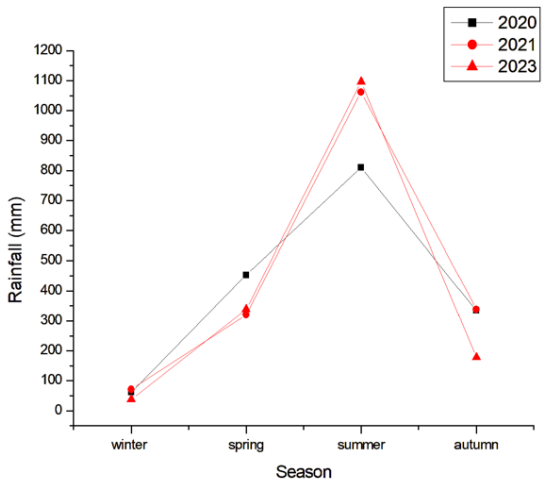

Figure 7. Graphic representation of the variation of seasonal rainfall for 2020, 2021 and 2023

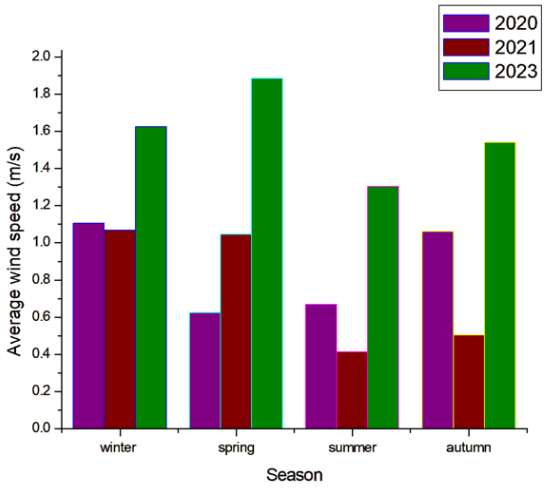

Figure 8. Graphic representation of the variation of seasonal average wind speed for 2020, 2021 and 2023

Climatic interpretation of model performance

The superior performance of higher-order models reflects the distinct climatic characteristics of Taplejung. Situated in the eastern Himalayan foothills, the region experiences:

- High atmospheric transparency during non-monsoon seasons
- Rapid cloud formation and dissipation
- Strong elevation-induced temperature gradients

These conditions necessitate empirical formulations capable of representing nonlinear interactions among meteorological variables. Sunshine duration alone proves inadequate, whereas hybrid models successfully capture the combined effects of temperature variability, relative humidity, and cloud dynamics.

The variation of monthly average daily GSR for 2020, 2021, and 2023 is presented in Figure 2**.** Figures 3 - 5 illustrate the comparison between measured and estimated daily GSR for the respective years, while Figures 6-8 depict the seasonal variation of GSR, rainfall, and average wind speed.

DISCUSSION

The results clearly indicate that empirical models developed for lowland or climatically homogeneous regions may not perform adequately in high-altitude mountainous environments such as Taplejung. Rapid atmospheric changes, complex cloud dynamics, and elevation-driven temperature variability significantly influence daily solar radiation.

The superior performance of multivariable and nonlinear models confirms the necessity of incorporating multiple meteorological parameters.

Sunshine duration alone fails to capture short-term variability, whereas hybrid formulations effectively represent the combined influence of temperature, humidity, and cloud cover.

The estimated mean daily GSR of approximately 15.12 MJ m^{-2} day^{-1} **(**≈ 4.2 kWh m^{-2} day^{-1}**)** confirms that Taplejung possesses substantial solar energy potential. This level of solar resource is suitable for decentralized photovoltaic systems, rural electrification, and micro-hybrid energy planning in mountainous regions where ground-based measurements are scarce.

Taplejung's annual mean global solar radiation (GSR) (15.12 MJ m^{-2} day^{-1} ≈ 4.2 kWh m^{-2} day^{-1}) is comparable to other eastern regions of Nepal (Rajbanshi et al., 2025c). It is slightly higher than Biratnagar (14.97 MJ m^{-2} day^{-1}) and very close to Dhankuta (15.10 MJ m^{-2} day^{-1}) and Okhaldhunga (15.17 MJ m^{-2} day^{-1}), showing similar solar energy potential across these areas (Rajbanshi et al., 2024a and 2024b; Rajbanshi et al., 2025a). In contrast, Jumla records much higher solar radiation (19.58 MJ m^{-2} day^{-1}), mainly due to its high altitude and clearer skies (Kharel et al., 2025). Kathmandu shows lower GSR (~13.55 MJ m^{-2} day^{-1}), which may be influenced by valley topography, air pollution, and frequent cloud cover (Dawadi et al., 2026).

Compared to international locations, Taplejung receives slightly higher solar radiation than New York City (14.07 MJ m^{-2} day^{-1}) and Hong Kong (13.52 MJ m^{-2} day^{-1}). However, it receives significantly less solar radiation than arid regions such as Cairo (19.92 MJ m^{-2} day^{-1}), Amman (20.51 MJ m^{-2} day^{-1}), and Juba (19.66 MJ m^{-2} day^{-1}), where clearer atmospheric conditions enhance solar irradiance (Al-Salameh et al., 2025; Deng et al., 2025).

CONCLUSION

This study presents a comprehensive evaluation of twenty empirical models for estimating daily global solar radiation in Taplejung, Nepal. Significant differences in predictive performance are observed, emphasizing the importance of site-specific model assessment in mountainous terrains. Among all tested formulations, the Coulibaly and Ouedraogo model (M20) emerges as the most reliable, exhibiting near-zero bias, low prediction error, and the highest correlation strength. Models Chen et al. model 2 (M16) and Ododo et al. Model (M17) also demonstrate strong performance and can serve as practical alternatives. Using multiple linear regression analysis, a site-specific empirical model based on the Coulibaly and Ouedraogo model (M20) was developed for Taplejung. The derived empirical constants are:

a = 2.8665, b = 0.03023, c = 11.1079, d = –0.100005, e = 0.6457, f = 1.01074

The proposed model is expressed as:

$$H_g = 2.8665 + 0.03023H_0 + 11.1079(n/N) - 0.100005(RH) + 0.6457T_{max} + 1.01074\sin\delta$$

The findings confirm that empirical modeling provides a cost-effective and reliable approach for solar radiation assessment in data-scarce mountainous regions. The identified optimal model can support solar energy planning and environmental studies in eastern Nepal and similar high-altitude areas.

ACKNOWLEDGMENTS

The authors express their sincere gratitude to the Department of Hydrology and Meteorology (DHM), Government of Nepal, for providing the necessary meteorological data used in this study.

AUTHORS CONTRIBUTION

Conceptualization: BKR; Methodology: RGS; Validation: BKR; Investigation: BKR; Data Analysis: BKR, RGS, AKSR; Writing original-draft: BKR; Writing-review & editing: BKR, RGS, AKSR, BKRC

FUNDING

None

ORCIDs

Basanta Kumar Rajbanshi:
https://orcid.org/0009-0003-7953-7475
Ram Gopal Singh:
http://orcid.org/0000-0003-3794-2088
Anima Kumari Singh Rajbanshi:
https://orcid.org/0009-0001-4159-818X

CONFLICT OF INTEREST

The authors declare that there is no conflict of interest regarding the publication of this paper.

ETHICAL STATEMENT

This study does not involve any human participants or animals. All data used in this research were obtained from authorized sources and used strictly for academic and research purposes.

DATA AVAILABILITY STATEMENT

The data of the present work will be made available by the corresponding author upon request.

SUPPLEMENTARY INFORMATION

None

REFERENCES

Adhikari, K. R., Gurung, S., & Bhattarai, B. K. (2013). Solar energy potential in Nepal and global

context. *Journal of the Institute of Engineering, 9*(1), 95–106. https://doi.org/10.3126/jie.v9i1.10675

Adhikari, K. R., Gurung, S., & Bhattarai, B. K. (2014). Empirical model based on meteorological parameters to estimate global solar radiation in Nepal. *BIBECHANA, 11*, 25–33. https://doi.org/10.3126/bibechana.v11i0.10376

Al-Salameh, A., et al. (2025). Assessment of long-term solar radiation for energy exploitation in East Jerusalem, Palestine. *International Journal of Energy and Environmental Science, 10*(4), 13. https://doi.org/10.11648/j.ijees.20251004.13

Ampratwum, D. B., & Dorvlo, A. S. S. (1999). Estimation of solar radiation from the number of sunshine hours. *Applied Energy, 63*, 161–167. https://doi.org/10.1016/S0306-2619(99)00025-2

Angstrom, A. (1924). Solar and terrestrial radiation: Report to the International Commission for Solar Research on actinometric investigations of solar and atmospheric radiation. *Quarterly Journal of the Royal Meteorological Society, 50*(210), 121–126. https://doi.org/10.1002/qj.49705021008

Badescu, V. (2008). *Modeling solar radiation at the Earth's surface*. Springer. https://doi.org/10.1007/978-3-540-77455-6

Chen, R., Ersi, K., Yang, J., Lu, S., & Zhao, W. (2004). Validation of five global radiation models with measured daily data in China. *Energy Conversion and Management, 45*(11–12), 1759–1769. https://doi.org/10.1016/j.enconman.2003.09.019

Dawadi, N., Shrestha, M. K., Khatri, K., Poudyal, K. N., Karki, I. B., & Tiwari, B. R. (2026). Estimation of global solar radiation using RadEst 3.00 software at Tribhuvan International Airport, Nepal. *BIBECHANA, 23*(1), 31–39. https://doi.org/10.3126/bibechana.v23i1.82026

Deng, J. M., Muot, D. Y., & Mawien, P. P. (2025). Uncovering South Sudan's renewable energy potential: A comprehensive evaluation of favourable locations and variability. *Energy, Sustainability and Society, 15*, 42. https://doi.org/10.1186/s13705-025-00542-y

Dogniaux, R., & Lemoine, M. (1983). Classification of radiation sites in terms of different indices of atmospheric transparency. In *Solar energy research and development in the European Community* (Series F, Vol. 2). Reidel. https://doi.org/10.1007/978-94-009-7112-7_7

Ertekin, C., & Yaldiz, O. (2000). Comparison of some existing models for estimating global solar radiation for Antalya (Turkey). *Energy Conversion and Management, 41*, 311–330. https://doi.org/10.1016/S0196-8904(99)00127-2

Evrendilek, F., & Ertekin, C. (2008). Assessing solar radiation models using multiple variables over Turkey. *Climate Dynamics, 31*, 131–149. https://doi.org/10.1007/s00382-007-0338-6

Gairaa, K., & Bakelli, Y. (2013). A comparative study of some regression models to estimate global solar radiation on a horizontal surface from sunshine duration and meteorological parameters for Ghardaïa site, Algeria. *International Scholarly Research Notices, 2013*, Article 754956. https://doi.org/10.1155/2013/754956

Glover, J., & McCulloch, J. S. G. (1958). The empirical relation between solar radiation and hours of sunshine. *Quarterly Journal of the Royal Meteorological Society, 84*, 172–175. https://doi.org/10.1002/qj.49708436011

Hamatti, M., Benchrifa, M., Elouardi, M., Hadine, M., Jamal, M., El-Baz, M., & Tadili, R. (2025). Prediction of daily global solar radiation on a horizontal plane using adaptive neuro-fuzzy inference system (ANFIS). *Journal of Environmental and Earth Sciences, 7*(1), 527–539. https://doi.org/10.30564/jees.v7i1.7079

Iqbal, M. (1983). *An introduction to solar radiation*. Academic Press. https://doi.org/10.1016/B978-0-12-373750-2.X5001-0

Joshi, U., Poudyal, K. N., Karki, I. B., & Chapagain, N. P. (2020). Evaluation of global solar radiation using sunshine hour, temperature, and relative humidity at lowland region of Nepal. *Journal of Nepal Physical Society, 6*(1), 16–24. https://doi.org/10.3126/jnphyssoc.v6i1.30429

Katiyar, A. K., & Pandey, C. K. (2010). Simple correlation for estimating global solar radiation on horizontal surfaces in India. *Energy, 35*, 5043–5048. https://doi.org/10.1016/j.energy.2010.08.014

Khalil, S. A., & Shaffie, A. M. (2014). The relationship between total solar radiation and biologically erythematic radiation over an urban region of Egypt. *Renewable and Sustainable Energy Reviews, 38*, 1092–1099. https://doi.org/10.1016/j.rser.2014.05.014

Kharel, B., Thapa, A., Khatiwada, K., Rijal, S., Rajbanshi, B. K., & Poudyal, K. N. (2025). Estimating solar energy potential in the high-altitude region of Jumla, Nepal, using RadEst 3.0 software. *Journal of Information Systems Engineering and Management, 10*(44s), 1013–1029. https://doi.org/10.52783/jisem.v10i44s.8698

Liou, K. N. (2002). *An introduction to atmospheric radiation*. Elsevier. https://www.sciencedirect.com/book/9780124514515/an-introduction-to-atmospheric-radiation

Liu, D. L., & Scott, B. J. (2001). Estimation of solar radiation in Australia from rainfall and temperature observations. *Agricultural and*

Forest Meteorology, 106, 41–59. https://doi.org/10.1016/S0168-1923(00)00173-8

Martínez-Lozano, J. A., Tena, F., Onrubia, J., & de la Rubia, J. (1984). The historical evolution of the Ångström formula and its modifications: Review and bibliography. *Agricultural and Forest Meteorology, 33*(2–3), 109–128. https://doi.org/10.1016/0168-1923(84)90064-9

Ögelman, H., Ecevit, A., & Taşdemiroğlu, E. (1984). A new method for estimating solar radiation from bright sunshine data. *Solar Energy, 33*(6), 619–625. https://doi.org/10.1016/0038-092X(84)90018-5

Okundamiya, M. S., Emagbetere, J. O., & Ogujor, E. A. (2016). Evaluation of various global solar radiation models for Nigeria. *International Journal of Green Energy, 13*(5), 505–512. https://doi.org/10.1080/15435075.2014.968921

Olomiyesan, B., Oyedum, O., Ugwuoke, P., & Abolarin, M. (2017). Evaluation of some global solar radiation models in selected locations in northwest Nigeria. *Open Access Journal of Photoenergy, 1*(1), 1–6. https://doi.org/10.15406/mojsp.2017.01.00001

Page, J. K. (1961). The estimation of monthly mean values of daily total shortwave radiation. *Proceedings of the UN Conference on New Sources of Energy, 4*, 378–390. https://digitallibrary.un.org/record/3827996?utm=&v=pdf

Poudyal, K. N. (2015). *Estimation of global solar radiation potential in Nepal* (Doctoral dissertation, Tribhuvan University, Institute of Engineering, Nepal).

Poudyal, K. N., Bhattarai, B. K., Sapkota, B. K., & Kjeldstad, B. (2012). Estimation of global solar radiation using sunshine duration in the Himalayan region. *Research Journal of Chemical Sciences, 2*(11), 20–25. https://www.isca.in/rjcs/Archives/v2/i11/4.ISCA-RJCS-2012-165.php?utm

Prescott, J. A. (1940). Evaporation from a water surface in relation to solar radiation. *Transactions of the Royal Society of South Australia, 64*, 114–118. https://www.scirp.org/reference/referencespapers?referenceid=4177006&utm

Rajbanshi, B. K., Singh, R. G., Khatiwada, K., Thapa, A., & K. C., B. R. (2024a). Comparative analysis of empirical models for estimating global solar radiation in Biratnagar, Nepal: A case study using RadEst 3.0. *Nanotechnology Perceptions, 20*(S16). https://nano-ntp.com/index.php/nano/article/view/4637

Rajbanshi, B. K., Singh, R. G., K. C., B. R., & Poudel, K. N. (2024b). Comparative analysis of different models within RadEst 3.0 for solar radiation estimation at Dhankuta, Nepal. *Journal of Nepal Physical Society, 10*(1), 70–76. https://doi.org/10.3126/jnphyssoc.v10i1.72845

Rajbanshi, B. K., Singh, R. G., Kharel, B., Thapa, A., & Khatiwada, K. (2025a). Estimation of solar energy using different empirical models at Okhaldhunga, Nepal. *International Journal of Environmental Science, 11*(7s), 92–102. https://doi.org/10.64252/v1y8pw19

Rajbanshi, B. K., Singh, R. G., K. C., B. R., Joshi, U., & Poudyal, K. N. (2025b). Determining the optimal empirical model for estimating global solar radiation in the eastern mid-hills of Dhankuta, Nepal. *Journal of Nepal Physical Society, 11*(1), 1–8. https://doi.org/10.3126/jnphyssoc.v11i1.87386

Rajbanshi, B. K., Singh, R. G., Khatiwada, K., Thapa, A., Kharel, B., & K C., B. R. (2025c). Estimation of global solar radiation in the eastern upland region of Taplejung, Nepal, using RadEst 3.0 software. *Journal of Information Systems Engineering and Management, 10*(16s). https://doi.org/10.52783/jisem.v10i16s.2658

Sonmete, M. H., Ertekin, C., Menges, H. O., Hacıseferogullari, H., & Evrendilek, F. (2011). Assessing monthly average solar radiation models: A comparative case study in Turkey. *Environmental Monitoring and Assessment, 175*, 251–277. https://doi.org/10.1007/s10661-010-1510-8

Tanyıldızı Ağır, T. (2025). Daily global solar radiation prediction with hybrid LSTM–SVM: The case of Nusaybin. *Arabian Journal for Science and Engineering*. Advance online publication. https://doi.org/10.1007/s13369-025-10322-7

Tarpley, J. D. (1979). Estimating incident solar radiation at the surface from geostationary satellite data. *Journal of Applied Meteorology and Climatology, 18*(9), 1172–1181. https://www.jstor.org/stable/26179173

Trnka, M., Žalud, Z., Eitzinger, J., & Dubrovský, M. (2005). Global solar radiation in Central European lowlands estimated by various empirical formulae. *Agricultural and Forest Meteorology, 131*, 54–76. https://doi.org/10.1016/j.agrformet.2005.05.002

Yadav, A. K., Kumar, R., Wang, M., Fekete, G., & Singh, T. (2025). Comparative analysis of daily global solar radiation prediction using deep learning models inputted with stochastic variables. *Scientific Reports, 15*, Article 10786. https://doi.org/10.1038/s41598-025-95281-7